

Stress field around arbitrarily shaped cracks in two-dimensional elastic materials

Version of November 10, 2018

Eran Bouchbinder¹, Joachim Mathiesen^{1,2} and Itamar Procaccia¹

¹*Dept. of Chemical Physics, The Weizmann Institute of Science, Rehovot 76100, Israel*

²*The Niels Bohr Institute, 17 Blegdamsvej, Copenhagen, Denmark*

The calculation of the stress field around an arbitrarily shaped crack in an infinite two-dimensional elastic medium is a mathematically daunting problem. With the exception of few exactly soluble crack shapes the available results are based on either perturbative approaches or on combinations of analytic and numerical techniques. We present here a general solution of this problem for any arbitrary crack. Along the way we develop a method to compute the conformal map from the exterior of a circle to the exterior of a line of arbitrary shape, offering it as a superior alternative to the classical Schwartz-Cristoffel transformation. Our calculation results in an accurate estimate of the full stress field and in particular of the stress intensity factors K_I and K_{II} and the T -stress which are essential in the theory of fracture.

I. INTRODUCTION

The existence of a crack in a stressed elastic medium does not necessarily mean that a catastrophic failure is in sight; otherwise many home owners would be in a constant state of panic. Indeed, one of the major objectives of the theory of fracture mechanics is to predict when the existence of a crack would necessarily lead to the failure of materials. A crucial ingredient of such a prediction is the determination of the state of deformation of a given material in the presence of the said crack under the effect of a given external loading. This calculation is not available for arbitrarily shaped cracks even in two dimensional elastic media. To explain the difficulty consider for a moment an existing crack in an infinite two dimensional medium. Under given load conditions the displacement field $\mathbf{u}(\mathbf{r}, t)$ is giving rise to the elastic strain tensor ϵ_{ij} :

$$\epsilon_{ij} \equiv \frac{1}{2} \left(\frac{\partial u_i}{\partial x_j} + \frac{\partial u_j}{\partial x_i} \right). \quad (1)$$

In linear elasticity the stress tensor is related to the strain tensor by [1]:

$$\sigma_{ij} = \frac{E}{1+\nu} \left(\frac{\nu}{1-2\nu} \delta_{ij} \sum_k \epsilon_{kk} + \epsilon_{ij} \right). \quad (2)$$

where E and ν are the Young's modulus and the Poisson's ratio respectively. When the boundary conditions at infinity include both opening and shear modes (with respect to the straight crack) the stress field near the tip of any crack has a universal form [2], i.e.

$$\sigma_{ij}(r, \varphi) = \frac{K_I}{\sqrt{2\pi r}} \Sigma_{ij}^I(\varphi) + \frac{K_{II}}{\sqrt{2\pi r}} \Sigma_{ij}^{II}(\varphi). \quad (3)$$

Here K_I and K_{II} are the "stress intensity factors" with respect to the opening and shear modes, whereas $\Sigma_{ij}^I(\varphi)$ and $\Sigma_{ij}^{II}(\varphi)$ are universal angular functions common to all configurations and loading conditions. Despite the simplicity of Eq. (3) the calculation of the stress intensity factors is not simple. Their numerical value depends on

the shape of the crack, its dynamical history and on the far field boundary conditions.

For a *straight* crack the stress intensity factors are known exactly [3, 4], i.e.

$$K_I = \sigma_{yy}^\infty \sqrt{\pi a}, \quad K_{II} = \sigma_{xy}^\infty \sqrt{\pi a}, \quad (4)$$

where $2a$ is the crack length and σ_{ij}^∞ is the uniform load at infinity. The criterion for failure is then the famous Griffith-Irwin criterion [5],

$$\frac{K_I^2 + K_{II}^2}{E} = \Gamma, \quad (5)$$

where Γ is the fracture energy. The physical meaning of Eq. (5) is that the crack will initiate (and may cause failure) when the elastic energy flowing from the stress field in the bulk to the tip region is at least as large as the energy lost by lengthening the crack (bond breaking or any other energy cost involved). In the case of the straight crack failure will occur, for a given level of the external load, at a critical crack length.

For cracks of arbitrary shape we still expect both Eqs. (3) and (5) to remain valid. The problem is then how to compute the stress intensity factors K_I and K_{II} when the crack is *not* straight. Indeed, a well known paper by Cotterell and Rice [6] offers such an analytic calculation for a *slightly curved* crack in perturbation theory in the amount of deviation from the straight crack. Many other works developed alternative hybrid numerical-analytical techniques like singular integral equations based either on dislocation distribution or crack "opening displacement functions" and superposition methods [7]. A large body of research is devoted to direct numerical techniques like the finite element method [8]. In this paper we offer a non-perturbative approach to the calculation of the *full* stress field of an arbitrarily shaped crack based on a conformal mapping technique. In particular, we will be able to estimate accurately the stress intensity factors and any other relevant quantities like the T -stress, a quantity to be defined below (cf. Eq. (40)). In Sect. 2 we lay out the mathematical problem. In Sect. 3 we present a solution based on the method of iterated conformal maps. This

section includes also the general problem of finding the conformal map from the unit circle to a line of an arbitrary shape. The section culminates in the calculation of the stress intensity factors. In Sect. 4 we exemplify the method and compare it against exactly soluble cases. Sect. 5 offers a short summary and a discussion.

II. MATHEMATICAL FORMULATION

The theory of elastostatic fracture mechanics in brittle continuous media is based on the equilibrium equations for an isotropic elastic body [1]

$$\frac{\partial \sigma_{ij}}{\partial x_j} = 0. \quad (6)$$

For in-plane modes of fractures, i.e. under plane-stress or plane-strain conditions, one introduces the Airy stress potential $U(x, y)$ such that

$$\sigma_{xx} = \frac{\partial^2 U}{\partial y^2}; \sigma_{xy} = -\frac{\partial^2 U}{\partial x \partial y}; \sigma_{yy} = \frac{\partial^2 U}{\partial x^2}. \quad (7)$$

Thus the set of Eq. (6), after simple manipulations, translate to a Bi-Laplace equation for the Airy stress potential $U(x, y)$ [1]

$$\Delta \Delta U(x, y) = 0, \quad (8)$$

with the prescribed boundary conditions on the crack and on the external boundaries of the material. At this point we choose to focus on the case of uniform remote loadings and traction-free crack boundaries. This choice, although not the most general, is of great interest and will serve to elucidate our method. Other solutions may be obtained by superposition. Thus, the boundary conditions at infinity, for the two in-plane symmetry modes of fracture, are presented as

$$\begin{aligned} \sigma_{xx}(\infty) = 0; \sigma_{yy}(\infty) = \sigma_\infty; \sigma_{xy}(\infty) = 0 & \quad \text{Mode I} \quad (9) \\ \sigma_{xx}(\infty) = 0; \sigma_{yy}(\infty) = 0; \sigma_{xy}(\infty) = \sigma_\infty & \quad \text{Mode II} \quad (10) \end{aligned}$$

In Addition, the free boundary conditions on the crack are expressed as

$$\sigma_{xn}(s) = \sigma_{yn}(s) = 0, \quad (11)$$

where s is the arc-length parametrization of the crack boundary and the subscript n denotes the out-ward normal direction.

The solution of the Bi-Laplace equation can be written in terms of *two* analytic functions $\phi(z)$ and $\eta(z)$ as

$$U(x, y) = \Re[\bar{z}\phi(z) + \eta(z)]. \quad (12)$$

In terms of these two analytic functions, using Eq. (7), the stress components are given by

$$\begin{aligned} \sigma_{yy}(x, y) &= \Re[2\phi'(z) + \bar{z}\phi''(z) + \eta''(z)] \\ \sigma_{xx}(x, y) &= \Re[2\phi'(z) - \bar{z}\phi''(z) - \eta''(z)] \\ \sigma_{xy}(x, y) &= \Im[\bar{z}\phi''(z) + \eta''(z)]. \end{aligned} \quad (13)$$

In order to compute the full stress field one should first formulate the boundary conditions in terms of the analytic functions $\phi(z)$ and $\eta(z)$ and to remove the gauge freedom in Eq. (12). The boundary conditions Eq. (11), using Eq. (7), can be rewritten as [3]

$$\partial_t \left[\frac{\partial U}{\partial x} + i \frac{\partial U}{\partial y} \right] = 0. \quad (14)$$

Note that we do not have enough boundary conditions to determine $U(x, y)$ uniquely. In fact we can allow in Eq. (12) arbitrary transformations of the form

$$\begin{aligned} \phi &\rightarrow \phi + iCz + \gamma \\ \psi &\rightarrow \psi + \tilde{\gamma}, \quad \psi \equiv \eta' \end{aligned} \quad (15)$$

where C is a real constant and γ and $\tilde{\gamma}$ are complex constants. This provides five degrees of freedom in the definition of the Airy potential. Two of these freedoms are removed by choosing the gauge in Eq. (14) according to

$$\frac{\partial U}{\partial x} + i \frac{\partial U}{\partial y} = 0, \quad \text{on the boundary} \quad (16)$$

It is important to stress that whatever the choice of the five freedoms, the stress tensor is unaffected; see [3] for an exhaustive discussion of this point. Computing Eq. (16) in terms of Eq. (12) we arrive at the boundary condition

$$\phi(z) + z\overline{\phi'(z)} + \overline{\psi(z)} = 0. \quad (17)$$

To proceed we represent $\phi(z)$ and $\psi(z)$ in Laurent expansion form:

$$\begin{aligned} \phi(z) &= \varphi_1 z + \varphi_0 + \varphi_{-1}/z + \varphi_{-2}/z^2 + \dots, \\ \psi(z) &= \psi_1 z + \psi_0 + \psi_{-1}/z + \psi_{-2}/z^2 + \dots \end{aligned} \quad (18)$$

This form is in agreement with the boundary conditions at infinity that disallow higher order terms in z . One freedom is now used to choose φ_1 to be real and two more freedoms will allow us later on to fix φ_0 . Then, using the boundary conditions (9) and (10), we find

$$\begin{aligned} \varphi_1 &= \frac{\sigma_\infty}{4}; \quad \psi_1 = \frac{\sigma_\infty}{2} \quad \text{Mode I}, \\ \varphi_1 &= 0; \quad \psi_1 = i\sigma_\infty \quad \text{Mode II}. \end{aligned} \quad (19)$$

III. THE SOLUTION

As said above, the direct determination of the stress tensor for a given arbitrary shaped crack is difficult. To overcome the difficulty we perform an intermediate step of determining the conformal map from the exterior of the unit circle to the exterior of our given crack. Currently the best available approach for such a task is the Schwartz-Cristoffel transformation. Here we will present an alternative new approach for finding the wanted conformal transformation, given in terms of a functional iteration of fundamental conformal maps. The use of iterated conformal maps was pioneered by Hastings and

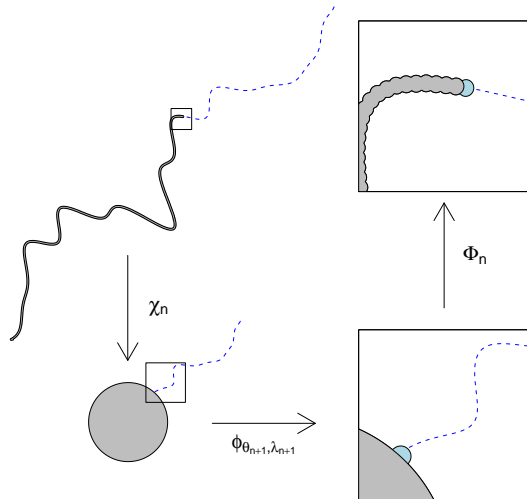


FIG. 1: Example of how to construct the conformal mapping along a line.

Levitov [9]; it was subsequently turned into a powerful tool for the study of fractal and fracture growth patterns [10, 11, 12, 13, 14, 15, 16]. In the next subsection we describe how, given a crack shape, to construct a conformal map from the complex w -plane to the physical z -plane such that the conformal map $z = \Phi(w)$ maps the exterior of the unit circle in the w -plane to the exterior of the crack in the physical z -plane, after n directed growth steps. We draw the reader's attention to the fact that this method is more general than its application in this paper, and in fact we offer it as a superior method to the Schwartz-Cristoffel transformation, with hitherto undetermined potential applications in a variety of two-dimensional contexts.

A. The conformal mapping

The essential building block in the present application, as in all the applications of the method of iterated conformal maps is the fundamental map $\phi_{\lambda, \theta}$ that maps the exterior circle onto the unit circle with a semi-circular bump of linear size $\sqrt{\lambda}$ which is centered at the point $e^{i\theta}$. This map reads [9]:

$$\phi_{0, \lambda}(w) = \sqrt{w} \left\{ \frac{(1 + \lambda)}{2w} (1 + w) \right. \quad (20)$$

$$\times \left[1 + w + w \left(1 + \frac{1}{w^2} - \frac{2}{w} \frac{1 - \lambda}{1 + \lambda} \right)^{1/2} \right] - 1 \left. \right\}^{1/2}$$

$$\phi_{\theta, \lambda}(w) = e^{i\theta} \phi_{0, \lambda}(e^{-i\theta} w). \quad (21)$$

The inverse mapping $\phi_{\theta=0, \lambda}^{-1}$ is of the form

$$\phi_{0, \lambda}^{-1} = \frac{\lambda z - \sqrt{1 + \lambda}(z^2 - 1)}{1 - (1 + \lambda)z^2} z. \quad (22)$$

By composing this map with itself n times with a judicious choice of series $\{\theta_k\}_{k=1}^n$ and $\{\lambda_k\}_{k=1}^n$ we will construct $\Phi^{(n)}(\omega)$ that will map the exterior of the circle to the exterior of an arbitrary simply connected shape. To understand how to choose the two series $\{\theta_k\}_{k=1}^n$ and $\{\lambda_k\}_{k=1}^n$ consider Fig. 1, and define the inverse map $\omega = \chi^{(n)}(z)$. Assume now that we already have $\Phi^{(n-1)}(\omega)$ and therefore also its analytic inverse $\chi^{(n-1)}(z)$ after $n - 1$ growth steps, and we want to perform the next iteration. To construct $\Phi^{(n)}(\omega)$ we advance our mapping in the direction of a point \tilde{z} in the z -plane by adding a bump in the direction of $\tilde{w} = \chi^{(n-1)}(\tilde{z})$ in the w -plane. The map $\Phi^{(n)}(\omega)$ is obtained as follows:

$$\Phi^{(n)}(\omega) = \Phi^{(n-1)}(\phi_{\theta_n, \lambda_n}(\omega)). \quad (23)$$

The value of θ_n is determined by

$$\theta_n = \arg[\chi^{(n-1)}(\tilde{z})] \quad (24)$$

The magnitude of the bump λ_n is determined by requiring fixed size bumps in the z -plane. This means that

$$\lambda_n = \frac{\lambda_0}{|\Phi^{(n-1)}(e^{i\theta_n})|^2}. \quad (25)$$

We note here that it is not necessary in principle to have fixed size bumps in the physical domain. In fact, adaptive size bumps could lead to improvements in the precision and performance of our scheme. We consider here the fixed size scheme for the sake of simplicity, and we will show that the accuracy obtained is sufficient for our purposes. Iterating the scheme described above we end up with a conformal map that is written in terms of an iteration over the fundamental maps (20):

$$\Phi^{(n)}(w) = \phi_{\theta_1, \lambda_1} \circ \dots \circ \phi_{\theta_n, \lambda_n}(w). \quad (26)$$

For the sake of newcomers to the art of iterated conformal maps we stress that this iterative structure is abnormal, in the sense that the order of iterates is inverted with respect to standard dynamical systems. On the other hand the inverse mapping follows a standard iterative scheme

$$\chi^{(n)}(z) = \phi_{\theta_n, \lambda_n}^{-1} \circ \dots \circ \phi_{\theta_1, \lambda_1}^{-1}(z). \quad (27)$$

The algorithm is then described as follows; first we divide the curve into segments separated by points $\{z_i\}$. The spatial extent of each segment is taken to be approximately $\sqrt{\lambda_0}$, in order to match the size of the bumps in the z -plane. Without loss of generality we can take one of these points to be at the center of coordinates and to be our starting point. From the starting point we now advance along the shape by mapping the next point z_i on the curve according to the scheme described above.

B. Solution in terms of conformal mappings

The conformal map $\Phi^{(n)}(\omega)$ is constructed in n iterative steps. For the discussion below we do not need the n superscript and will denote simply $\Phi(\omega) \equiv \Phi^{(n)}(\omega)$. This map is univalent [10], having the Laurent expansion form

$$\Phi(\omega) = F_1\omega + F_0 + F_{-1}/\omega + F_{-2}/\omega^2 + \dots \quad (28)$$

Any position z in the physical domain is mapped by $\chi(z) \equiv \Phi^{-1}(z)$ onto a position ω in the mathematical domain. This transformation does not immediately provide the solution as the Bi-Laplacian operator, in contrast to the Laplacian operator, is not conformally invariant. Nevertheless, the conformal mapping method can be extended to non-Laplacian problems. We begin by writing our unknown functions $\varphi(z)$ and $\psi(z)$ in terms of the conformal map

$$\varphi(z) \equiv \tilde{\varphi}(\chi(z)) \quad , \quad \psi(z) \equiv \tilde{\psi}(\chi(z)) \quad . \quad (29)$$

Using the Laurent form of the conformal map, Eq. (28), the linear term as $\omega \rightarrow \infty$ is determined by Eqs. (29). We therefore write

$$\begin{aligned} \tilde{\varphi}(\omega) &= \varphi_1 F_1 \omega + \tilde{\varphi}_{-1}/\omega + \tilde{\varphi}_{-2}/\omega^2 + \dots \quad , \\ \tilde{\psi}(\omega) &= \psi_1 F_1 \omega + \tilde{\psi}_0 + \tilde{\psi}_{-1}/\omega + \tilde{\psi}_{-2}/\omega^2 + \dots \quad , \end{aligned} \quad (30)$$

where we used the last two freedoms to choose $\varphi_0 = -F_0\varphi_0$ such that $\tilde{\varphi}_0 = 0$. The boundary condition (17) is now read for the unit circle in the ω -plane. Denoting $\epsilon \equiv e^{i\theta}$ and

$$u(\epsilon) \equiv \sum_{n=1}^{\infty} \tilde{\varphi}_{-n}/\epsilon^n \quad , \quad v(\epsilon) \equiv \sum_{n=0}^{\infty} \tilde{\psi}_{-n}/\epsilon^n \quad , \quad (31)$$

we write

$$u(\epsilon) + \frac{\Phi(\epsilon)}{\Phi'(\epsilon)} \overline{u'(\epsilon)} + \overline{v(\epsilon)} = f(\epsilon) \quad . \quad (32)$$

The function $f(\epsilon)$ is a known function that contains all the coefficients that were determined so far:

$$f(\epsilon) = -\varphi_1 F_1 \epsilon - \frac{\Phi(\epsilon)}{\Phi'(\epsilon)} \varphi_1 F_1 - \frac{\overline{\psi_1 F_1}}{\epsilon} \quad . \quad (33)$$

To solve the problem we need to compute the coefficients $\tilde{\varphi}_n$ and $\tilde{\psi}_n$. To this aim we first write [15]

$$\frac{\Phi(\epsilon)}{\Phi'(\epsilon)} = \sum_{-\infty}^{\infty} b_i \epsilon^i \quad . \quad (34)$$

The function $f(\epsilon)$ has also an expansion of the form

$$f(\epsilon) = \sum_{-\infty}^{\infty} f_i \epsilon^i \quad . \quad (35)$$

In the discussion below we assume that the coefficients b_i and f_i are known. In order to compute these coefficients

we need to Fourier transform the function $\Phi(\epsilon)/\overline{\Phi'(\epsilon)}$. This is the most expensive step in our solution. One needs to carefully evaluate the Fourier integrals between the branch cuts. Using the last two equations together with Eqs. (31) and (32) we obtain

$$\tilde{\varphi}_{-m} - \sum_{k=1}^{\infty} k b_{-m-k-1} \tilde{\varphi}_{-k}^* = f_{-m} \quad , \quad m = 1, 2, \dots \quad (36)$$

$$\tilde{\psi}_{-m}^* - \sum_{k=1}^{\infty} k b_{m-k-1} \tilde{\varphi}_{-k}^* = f_m \quad . \quad m = 0, 1, 2, \dots \quad (37)$$

These sets of linear equations are well posed. The coefficients $\tilde{\varphi}_{-m}$ can be calculated from equation (36) alone, and then they can be used to determine the coefficients $\tilde{\psi}_{-m}$. This is in fact a proof that Eq. (32) determines the functions $u(\epsilon)$ and $v(\epsilon)$ together. This fact had been proven with some generality in [3].

The calculation of the Laurent expansion form of $\tilde{\varphi}(\omega)$ and $\tilde{\psi}(\omega)$ provides the solution of the problem in the ω -plane. Still, one should express the derivatives of $\varphi(z)$ and $\eta(z)$ in terms of $\tilde{\varphi}(\omega)$ and $\tilde{\psi}(\omega)$ and the inverse map $\chi(z)$ to obtain the solution in the physical z -plane. This is straight forward and yields

$$\begin{aligned} \varphi'(z) &= \tilde{\varphi}'[\chi(z)] \chi'(z) \\ \varphi''(z) &= \tilde{\varphi}''[\chi(z)] [\chi'(z)]^2 + \tilde{\varphi}'[\chi(z)] \chi''(z) \\ \eta''(z) &= \psi'(z) = \tilde{\psi}'[\chi(z)] \chi'(z) \end{aligned} \quad (38)$$

Upon substituting these relations into Eq. (13) one can calculate the *full* stress field for an arbitrarily shaped crack. The expression of the stress field in terms of the inverse conformal mapping is known for quite a long time although it is very limited as the conformal mapping and its inverse is rarely at hand. The central step of progress in this paper is the conjunction of the novel functional iterative scheme for obtaining the inverse conformal mapping with the known result that expresses the stress field in terms of this inverse mapping.

C. The Stress Intensity Factors and the T-stress

Linear elasticity fracture mechanics, under small scale yielding, has no intrinsic length scale. Accordingly the stress intensity factors are the most important quantities that characterize the universal near-tip fields. At this point we explain how to calculate the stress intensity factors from our solution.

In principle, the calculation follows directly from the solution in terms of the conformal map as described above. Previous authors derived the following expression for the complex combination (of the real) stress intensity factors [17]:

$$K_I - iK_{II} = 2\sqrt{\frac{\pi}{e^{i\delta_j} \Phi''(\omega_j)}} \tilde{\varphi}'(\omega_j) \quad , \quad (39)$$

where ω_j is the position of the tip in the ω -plane, and δ_j is the argument of the tip position z_j in the physical plane. This result, although exact, cannot be used to obtain accurate estimates of the stress intensity factors in our method. Since we construct our crack from a succession of little bumps, our crack tip is not infinitely sharp. Therefore we cannot base our calculation of the stress intensity factors on the precise coordinates of the tip. Rather, we need to exploit our knowledge of the stress field for a substantial region around the tip. We thus consider the stress field in the region of the tip, and write the components along the tangent to the crack at the tip [2]

$$\begin{aligned}\sigma_{\varphi\varphi}(r, 0) &= \frac{K_I}{\sqrt{2\pi r}} + b_{\varphi\varphi}\sqrt{r} \\ \sigma_{r\varphi}(r, 0) &= \frac{K_{II}}{\sqrt{2\pi r}} + b_{r\varphi}\sqrt{r} \\ \sigma_{rr}(r, 0) &= \frac{K_I}{\sqrt{2\pi r}} + T + b_{rr}\sqrt{r}.\end{aligned}\quad (40)$$

We have added terms of $O(\sqrt{r})$ to the leading terms, and in addition we took into account the T -stress contribution to the purely radial component σ_{rr} . It is crucial to note that there are no other $O(1)$ terms in the first two lines of Eq. (40). We did not need to consider explicitly any higher $O(r^{3/2})$ terms. In order to extract the stress intensity factors from the full field distributions we fit our solution near the tip to the form given by Eq. (40). We thus obtain not only the stress intensity factors but also the coefficient of the subleading terms. We note that the so-called T -stress has an important role in fracture theory (cf. [2, 4, 6]).

IV. DEMONSTRATIONS OF THE METHOD

In this section we demonstrate our method for two (of the very rare) exactly soluble geometries. There are many numerically solved problems in the literature that one can use for comparison, but our aim here is to exemplify the essentials of our approach. We will see that the method works very well and we propose that it can be used for arbitrary crack shapes as well.

A. The Straight Crack

The problem of a crack of length $2a$ in an infinite domain, subjected to a remote uniaxial load $\sigma_{yy} = \sigma^\infty$ and traction-free crack faces is considered as the canonical problem in the theory of linear elasticity fracture mechanics. The resulting stress field is known, and is given by [4]:

$$\sigma_{yy}(x, y) = \sigma^\infty \Re \left[\frac{z}{\sqrt{z^2 - a^2}} + \frac{iy a^2}{(z^2 - a^2)^{3/2}} \right]$$

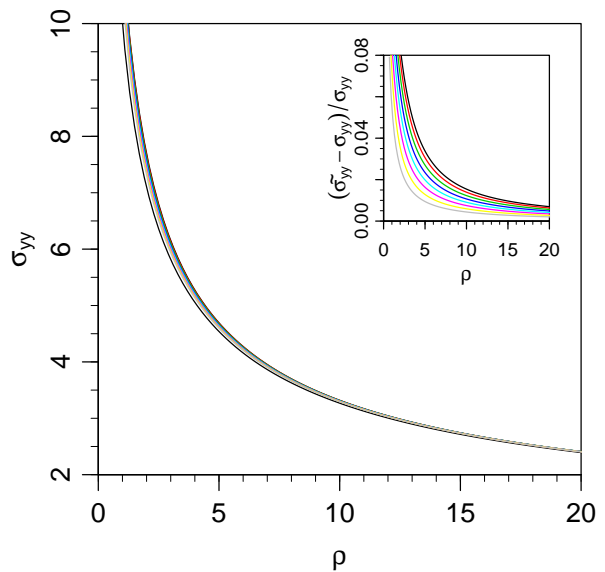


FIG. 2: The stress tensor component σ_{yy} for a straight crack with $a = 200$. The component is evaluated for $y = 0$ and a distance ρ away from the tip at $x = 200$. The numerical estimates $\tilde{\sigma}_{yy}$ approaches the analytical result (the left most line) as we decrease the linear size of the bumps $\sqrt{\lambda_0} = 1.0, 0.9, 0.8, \dots, 0.3$. The inset shows the relative error.

$$\begin{aligned}\sigma_{xx}(x, y) &= \sigma^\infty \Re \left[\frac{z}{\sqrt{z^2 - a^2}} - \frac{iy a^2}{(z^2 - a^2)^{3/2}} \right] - \sigma^\infty \\ \sigma_{xy}(x, y) &= -\sigma^\infty \Re \left[\frac{y a^2}{(z^2 - a^2)^{3/2}} \right],\end{aligned}\quad (41)$$

where $z = x + iy$ and the crack is represented by a branch cut along $-a < x < a$, $y = 0$.

We applied our general solution to the straight crack problem. We constructed the conformal mapping using our functional iteration scheme although the exact conformal mapping is known to be

$$\Phi(\omega) = \frac{a}{2} \left(\omega + \frac{1}{\omega} \right).\quad (42)$$

Fig. 2 compares our calculation of σ_{yy} along the x -axis with the exact result. The deviation near the tip of the crack is expected as in our solution the crack tip is not infinitely sharp but has a finite radius of curvature controlled by the parameter λ in Eq. (20). Decreasing the value of λ , we can obtain more accurate results. Note that real crack-tips *do* have a finite radius of curvature, so that our method can be even more appropriate; the idealization of representing cracks by mathematical branch cuts is no longer a necessary simplification.

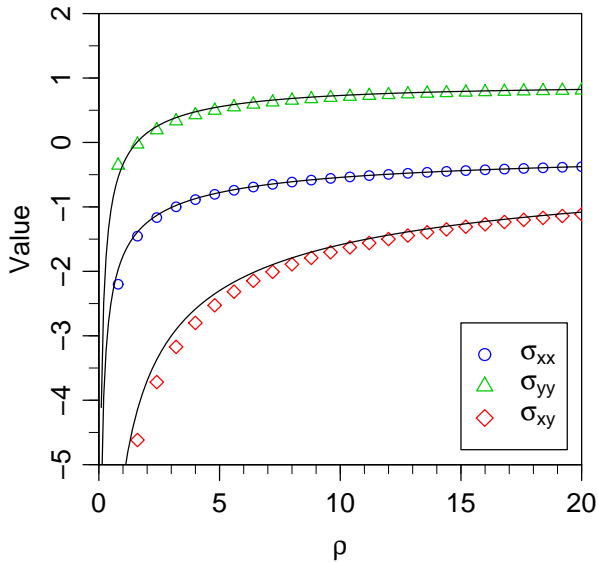


FIG. 3: The stress tensor components along the tangent to the crack tip. The crack is a semi circular arc of radius 200. ρ is the distance away from the tip. The points show the numerical values computed using bumps of linear size $\sqrt{\lambda_0} = 0.6$ and the lines are the corresponding analytical values.

B. The Circular Arc Crack

The analytic methods developed by Muskhelishvili [3] lead to the solution of various problems concerned with circular regions and infinite regions cut along circular arcs. Here we consider a crack in the shape of a circular arc that extends from $z = e^{i\theta}$ to $z = e^{-i\theta}$. This crack is subjected to a remote uniaxial load $\sigma_{xx} = \sigma^\infty$ parallel to the x -axis with traction-free crack boundaries. The stress tensor components are calculated from Eq. (13) with [3]

$$\begin{aligned} \varphi'(z) &= \frac{\sigma_\infty}{2G(z)} \left[C(\theta)(z - \cos(\theta)) + \frac{\cos(\theta)}{2z} - \frac{1}{2z^2} \right] \\ &+ \sigma_\infty \left[\frac{1}{4} - \frac{C(\theta)}{2} - \frac{1}{4z^2} \right] \\ \Omega(z) &= \frac{\sigma_\infty}{2G(z)} \left[C(\theta)(z - \cos(\theta)) + \frac{\cos(\theta)}{2z} - \frac{1}{2z^2} \right] \\ &- \sigma_\infty \left[\frac{1}{4} - \frac{C(\theta)}{2} - \frac{1}{4z^2} \right] \\ \psi'(z) &= \frac{\varphi'(z)}{z^2} - \frac{\bar{\Omega}(1/z)}{z^2} - \frac{\varphi''(z)}{z}. \end{aligned} \quad (43)$$

Here

$$\begin{aligned} C(\theta) &= \frac{1 - \sin^2(\theta/2) \cos^2(\theta/2)}{2[1 + \sin^2(\theta/2)]} \\ G(z) &= \sqrt{z^2 - 2z \cos(\theta) + 1}, \end{aligned} \quad (44)$$

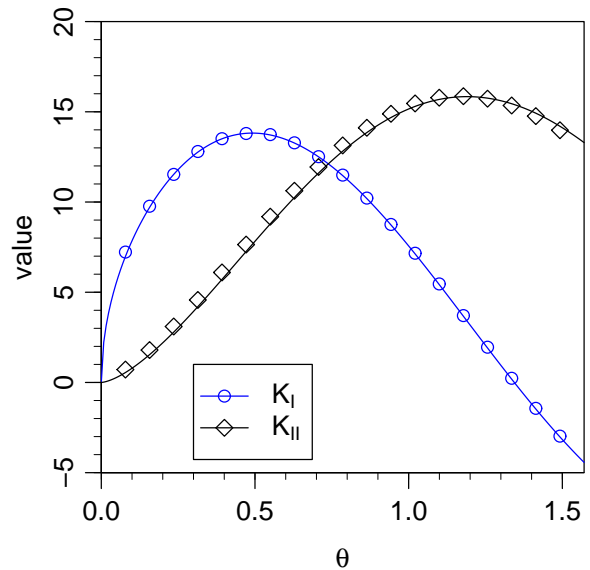


FIG. 4: Stress intensity factors for circular arcs of angles 2θ . The points are the numerical values computed from fitting of the stress field along the tangent to the crack tip. The fitting function used is of the form Eq. (40). In this calculation $\sqrt{\lambda_0} = 0.4$, and the fitting window is $5 < \rho < 30$.

where $G(z)$ is defined such that $z^{-1}G(z) \rightarrow 1$ as $z \rightarrow \infty$, which leads to $G(0) = -1$. Note that these results are given for an arc of unit radius and therefore the solution for any other circular arc can be obtained by a suitable rescaling transformation.

We applied our method for this configuration. The results for all the three components of the stress tensor field for $\theta = \pi/2$ along the continuation of the tip parallel to the x -axis are presented in Fig. 3 and compared with the exact results.

Finally, we used the method to extract the stress intensity factors. Fig. 4 shows the mode I and mode II stress intensity factors as a function of the half arc angle θ and compares them with the exact analytic result derived from the full field solution [4].

V. SUMMARY AND CONCLUSIONS

In summary, we have demonstrated that the method of iterated conformal maps can be used to construct the conformal map from the exterior of the unit circle to the exterior of an arbitrary crack. Next one can address the calculation of the stress field around such a crack with given loads at infinity. Having the said conformal map at hand simplifies enormously the calculation of the full stress field, allowing an accurate estimate of the stress intensity factors or of the sub-leading terms like the T -stress. The method was demonstrated by comparison with exactly soluble examples. The quality of the comparison leads to the conclusion that the issue of potential

failure of a material given a crack and boundary conditions can be efficiently dealt with. Future work will employ the present method to describe the dynamics of slow fracture where quasi-static methods are adequate.

Acknowledgments

This work had been supported in part by European Commission under a TMR grant.

-
- [1] L.D. Landau and E.M. Lifshitz, *Theory of Elasticity*, 3rd ed. (Pergamon, London, 1986).
- [2] L. B. Freund, *Dynamic Fracture Mechanics*, (Cambridge, 1998)
- [3] N. I. Muskhelishvili, *Some Basic Problems of the Mathematical Theory of Elasticity*, (Noordhoff, 1953).
- [4] K. B. Broberg, *Cracks and Fracture*, (Academic Press, 1999).
- [5] G. R. Irwin, *J. App. Mech.* **24**, 361 (1957).
- [6] B. Cotterell and J. R. Rice, *Int. J. Fract.* **16**, 155 (1980).
- [7] The number of publications on this problem is enormous. See for example, Y. Z. Chen, *Eng. Fract. Mech.* **51**, 97 (1995); *Theor. Appl. Fract. Mech.* **31**, 223 (1999); J. K. Burton and S. L. Phoenix, *Int. J. Fract.* **102**, 99 (2000).
- [8] See for example C. Daux, N. Moës, John Dolbow, N. Sukumar and T. Belytschko, *Int. J. Numer. Meth. Engng.* **48**, 1741 (2000).
- [9] M.B. Hastings and L.S. Levitov, *Physica D* **116**, 244 (1998).
- [10] B. Davidovitch, H.G.E. Hentschel, Z. Olami, I. Procaccia, L.M. Sander, and E. Somfai, *Phys. Rev. E*, **59** 1368 (1999).
- [11] B. Davidovitch, M.J. Feigenbaum, H.G.E. Hentschel and I. Procaccia, *Phys. Rev. E* **62**, 1706 (2000).
- [12] B. Davidovitch, A. Levermann, I. Procaccia, *Phys. Rev. E*, **62** R5919.
- [13] B. Davidovitch, M. H. Jensen, A. Levermann, J. Mathiesen and I. Procaccia, *Phys. Rev. Lett.* **87**, 164101 (2001).
- [14] F. Barra, B. Davidovitch, A. Levermann and I. Procaccia, *Phys. Rev. Lett.* **87**, p. 134501 (2001).
- [15] F. Barra, A. Levermann and I. Procaccia, *Phys. Rev. E.*, **66**, 066122 (2002).
- [16] A. Levermann and I. Procaccia, *Phys. Rev. Lett.*, **89**, 234501 (2002).
- [17] H. Andersson, *J. Mech. Phys. Solids* **17**, 417 (1969).